

Comprehensive Evaluation of Fourteen Docking Programs on Protein–Peptide Complexes

Gaoqi Weng, Junbo Gao, Zhe Wang, Ercheng Wang, Xueping Hu, Xiaojun Yao, Dongsheng Cao,* and Tingjun Hou*

Cite This: *J. Chem. Theory Comput.* 2020, 16, 3959–3969

Read Online

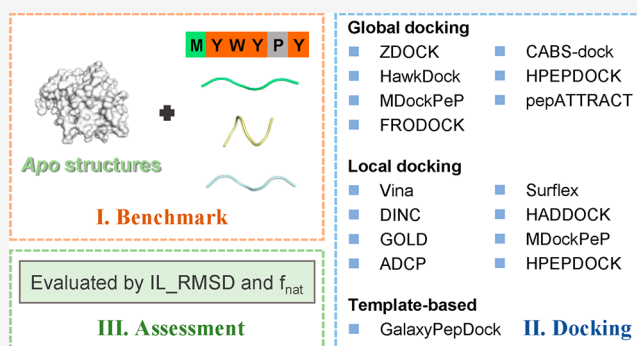
ACCESS |

Metrics & More

Article Recommendations

Supporting Information

ABSTRACT: A large number of protein–protein interactions (PPIs) are mediated by the interactions between proteins and peptide segments binding partners, and therefore determination of protein–peptide interactions (PpIs) is quite crucial to elucidate important biological processes and design peptides or peptidomimetic drugs that can modulate PPIs. Nowadays, as a powerful computation tool, molecular docking has been widely utilized to predict the binding structures of protein–peptide complexes. However, although a number of docking programs have been available, the systematic study on the assessment of their performance for PpIs has never been reported. In this study, a benchmark data set called PepSet consisting of 185 protein–peptide complexes with peptide length ranging from 5 to 20 residues was employed to evaluate the performance of 14 docking programs, including three protein–protein docking programs (ZDOCK, FRODOCK, and HawkDock), three small molecule docking programs (GOLD, Surflex-Dock, and AutoDock Vina), and eight protein–peptide docking programs (GalaxyPepDock, MDockPeP, HPEPDOCK, CABS-dock, pepATTRACT, DINC, AutoDock CrankPep (ADCP), and HADDOCK peptide docking). A new evaluation parameter, named IL_RMSD, was proposed to measure the docking accuracy with f_{nat} (the fraction of native contacts). In global docking, HPEPDOCK performs the best for the entire data set and yields the success rates of 4.3%, 24.3%, and 55.7% at the top 1, 10, and 100 levels, respectively. In local docking, overall, ADCP achieves the best predictions and reaches the success rates of 11.9%, 37.3%, and 70.3% at the top 1, 10, and 100 levels, respectively. It is expected that our work can provide some helpful insights into the selection and development of improved docking programs for PpIs. The benchmark data set is freely available at <http://cadd.zju.edu.cn/pepset/>.



INTRODUCTION

Protein–protein interactions (PPIs) are involved in various biological processes, and a significant number of PPIs are mediated by the interactions between proteins and peptides.¹ It has been estimated that protein–peptide interactions (PpIs) account for about 15–40% of the PPIs within the cell.¹ Elucidating the structural details of protein–peptide complexes is fundamental for the understanding of the molecular mechanisms underlying protein–peptide recognition and the development of peptide therapeutics. However, experimental characterization of protein–peptide complex structures is greatly impeded by the highly dynamic and transient nature of PpIs. Therefore, as important alternatives to complement experimental technologies, a variety of computational methods, especially protein–peptide docking, have been developed to predict the binding structures of protein–peptide complexes.

Current protein–peptide docking algorithms can be roughly divided into two classes: template-based docking and template-free docking.² Template-based docking methods predict the binding structures of protein–peptide complexes using the

structures of similar complexes as the templates, such as GalaxyPepDock.³ Although several successes have been achieved, templated-based docking methods suffer from the limited known templates, thus resulting in an innate limitation for general applications. In contrast, template-free docking does not need any template, and it can be subdivided into global docking and local docking on the basis of whether the binding site is known or not. Global docking executes an exhaustive search on the entire surface of the protein to capture the binding site and binding mode of the peptide, such as pepATTRACT,⁴ MDockPeP,⁵ CABS-dock,⁶ ClusPro PeptiDock,⁷ PIPER-FlexPepDock,⁸ and HPEPDOCK.⁹ However, local docking searches the binding poses of the peptide around the user-

Received: December 5, 2019

Published: April 23, 2020



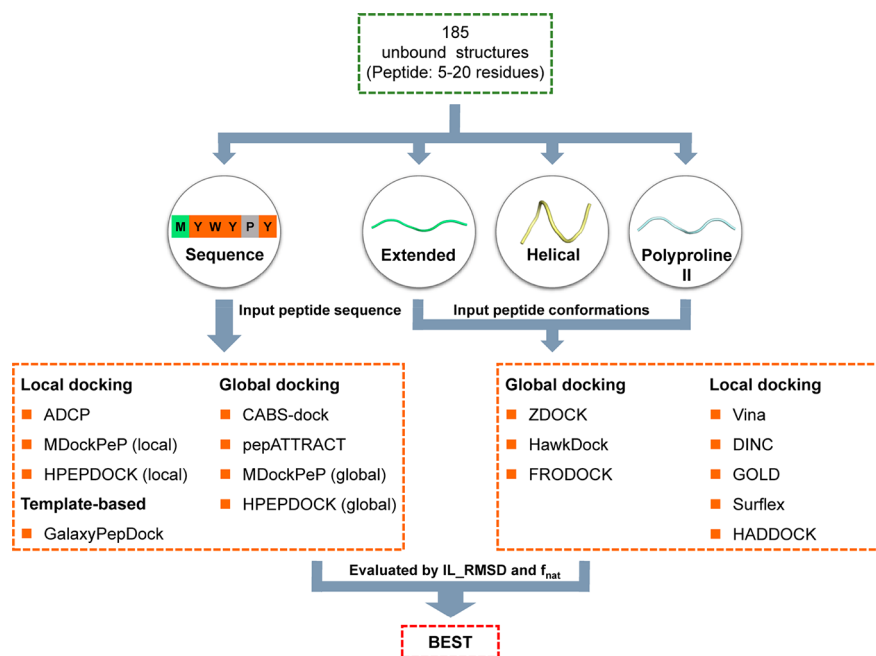


Figure 1. Overview of this study. For docking programs requiring the peptide structures as the input, three initial peptide conformations and unbound proteins were used for docking. For the other docking programs, only the peptide sequence and unbound proteins were employed for docking. Subsequently, the success rates of each programs were evaluated by IL_RMSD and f_{nat} .

defined binding site. The representative local docking methods include AutoDock Vina (Vina),¹⁰ GOLD,¹¹ Surflex-Dock (Surflex),¹² DynaDock,¹³ HADDOCK peptide docking (HADDOCK),¹⁴ PEP-FOLD 3,¹⁵ DINC,¹⁶ and AutoDock CrankPep (ADCP).¹⁷ Moreover, it is warranted to mention that ADCP can also handle the docking of the cyclic peptides.¹⁸

Although a number of docking programs have been developed, there is still a lack of a systematic evaluation to reveal the advantages and limitations of these docking programs for protein–peptide systems. As far as we know, only two simple comparative studies have been reported. Hauser and Windshügel assessed four small molecule docking programs on the basis of a data set that consists of 53 protein–peptide complexes with the peptide length ranging from 3 to 12 residues.¹⁹ Agrawal et al. evaluated five protein–protein docking programs and pepATTRACT on the basis of 133 protein–peptide complexes whose peptide lengths range from 9 to 15 residues.²⁰ In both of these studies, the evaluated docking programs only contained one protein–peptide docking program, and the bound structures were used in assessment. However, peptides are usually docked to the unbound proteins in reality, and the unbound proteins may undergo some conformational change upon the peptide binding. Moreover, the initial peptide conformations used in these two studies are the linear conformations (backbone torsion angles of 180°) and cocrystallized peptide structures. It is obvious that, considering the highly dynamic nature of peptides and the limitation of sampling algorithms, the initial peptide conformations have non-negligible impacts on the prediction accuracy of protein–peptide docking, especially rigid-body docking algorithms. Apart from the evaluation based on the benchmark, CAPRI (Critical Assessment of Predicted Interactions),²¹ the famous blind assessment of protein–protein docking, also releases a number of protein–peptide complexes. However, since 2013, only ten protein–peptide targets (rounds 28, 29, 38, and 44) were evaluated altogether, which cannot meet the demands of the

rapid development of protein–peptide docking algorithms. Additionally, a number of groups introduced some customized methods to optimize the docking results in CAPRI.²² However, it is difficult for docking program end-users to implement these customized methods. Thus, there is an urgent need to comprehensively assess the performance of protein–peptide docking algorithms on the basis of an extensive benchmark.

In this study, in order to systematically assess the performance of docking programs, a large benchmark called PepSet composed of 185 protein–peptide complexes with peptide lengths ranging from 5 to 20 residues was constructed. A total of 14 docking programs including three for protein–protein docking, three for small molecule–protein docking, and eight for protein–peptide docking were evaluated on the basis of this benchmark. Considering the remarkable influence of the initial peptide conformations on docking performance, three initial conformations (helical, extended, and polyproline II) were generated for the docking programs that require the peptide structures as the input. Besides, different from the common evaluation metrics of the interface root-mean-square-deviation (I_RMSD) or ligand RMSD (L_RMSD), a new evaluation parameter named IL_RMSD was proposed and employed to assess the performance of docking programs. Meanwhile, f_{nat} , the fraction of native contacts, was also used to assess the prediction quality for the side chains of peptides. The overview of this study is shown in Figure 1.

MATERIALS AND METHODS

Benchmark Data Set. PepSet was extracted from PepBDB,²³ which collected all the protein–peptide complexes with peptide lengths up to 50 amino acids from the Protein Data Bank.²⁴ The extraction criteria are as follows: (1) the peptide length ranges from 5 to 20 residues; (2) the resolution is $\leq 2.0 \text{ \AA}$; (3) peptides do not contain any nonstandard amino acid; (4) the sequence identity between any two protein monomers that interact directly with peptides is $< 30\%$; (5) the bound structures

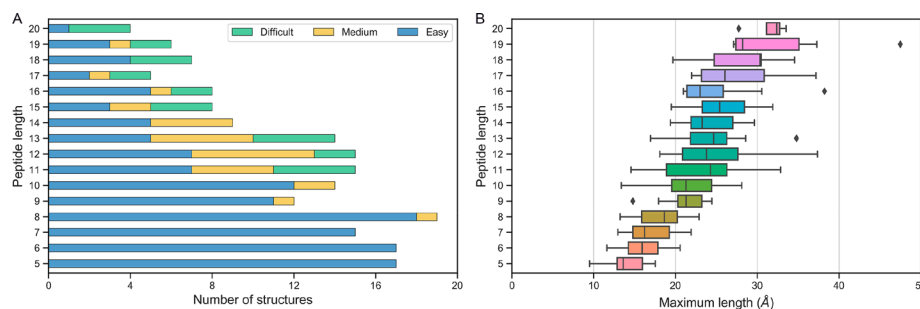


Figure 2. (A) Distribution of the protein–peptide complexes grouped by peptide length and difficulty. (B) The box plot of the variation of the maximum length, which includes the minimum, the first quartile (Q1), the sample median, the third quartiles (Q3) and the maximum. The minimum and the maximum are the lowest and largest data points excluding outliers. If a data point is lower than $Q1 - 1.5 \times IQR$ ($IQR = Q3 - Q1$) or larger than $Q3 + 1.5 \times IQR$, it will be plotted as an outlier. The maximum length is the maximum value in $((x_{\max} - x_{\min}), (y_{\max} - y_{\min}), (z_{\max} - z_{\min}))$. Here, $x, y,$ and z represent the atomic coordinates of the cocrystallized peptide in the three dimensions, respectively. The different colors are only used to distinguish data.

Table 1. Overview of the 14 Assessed Docking Programs

program	type ^a	required input ^b	sampling algorithm	scoring function
GalaxyPepDock	Pp, T	N/A	(i) select templates based on structure and interaction similarity; (ii) build model by energy-based optimization	energy-based scoring function
ZDOCK	PP, G	Pc	fast Fourier transform correlation algorithm	shape complementarity, electrostatic potential, and knowledge-based pair potentials
FRODOCK	PP, G	Pc	spherical Fourier transform correlation algorithm	van der Waals, electrostatic, and desolvation potentials and knowledge-based pair potentials
HawkDock	PP, G	Pc	ATTRACT: randomized search algorithm	van der Waals, electrostatic, and desolvation potentials
MDockPeP	Pp, G, L	N/A	modified version of Vina: iterated local search global optimizer	ITScorePeP: statistical potential-based scoring function
HPEPDOCK	Pp, G, L	N/A	modified version of MDOCK: an ensemble docking algorithm	iterative knowledge-based scoring function
CABS-dock	Pp, G	N/A	replica exchange Monte Carlo dynamics	clustering-based scoring function
pepATTRACT	Pp, G	N/A	ATTRACT: randomized search algorithm	Lennard-Jones type potentials and electrostatics
GOLD	SM, L	Pc	genetic algorithm	GoldScore: protein–ligand hydrogen bond and van der Waals energies, ligand internal van der Waals and torsional strain energies
Surflex-Dock	SM, L	Pc	incremental docking algorithm	empirical Hammerhead scoring function
AutoDock Vina	SM, L	Pc	iterated local search global optimizer	empirical scoring function
DINC	Pp, L	Pc	incremental docking algorithm based on AutoDock or Vina	scoring function of AutoDock or Vina
AutoDock CrankPep	Pp, L	N/A	CRANKITE: Metropolis Monte Carlo search	CRANKITE's $G\ddot{o}$ -type potential, Ramachandran propensities, and AutoDock affinity grids
HADDOCK peptide docking	Pp, L	Pc	randomized search algorithm	bond, angle, torsional angle, and electrostatic, van der Waals, and desolvation potentials

^aPp: protein–peptide docking. PP: protein–protein docking. SM: small molecule docking. G: global docking. L: locking docking. T: template-based modeling. ^bN/A: programs do not require the initial peptide conformation as the input. Pc: programs require the initial peptide conformation as the input.

have the corresponding unbound receptor structures and their sequence identity is >90%; (6) the RMSD of the backbone atoms of the residues in the bound structures within 10 Å from the peptide and the corresponding residues in the unbound structures is ≤ 2.0 Å. A total of 188 PDB entries were extracted on the basis of these criteria. After we examined the unbound and bound structures carefully, two complexes were removed because some important residues around the binding sites in the unbound structures were missing in the bound structures. Another structure had several missing residues in the middle of peptide that have not been resolved. At last, 185 out of the 188 complexes were incorporated into the final data set (Table S1 and Figure 2A,B). The benchmark data set is freely available at <http://cadd.zju.edu.cn/pepset/>.

Benchmark Classification. In terms of the RMSD of the backbone atoms between the conformation of the peptide in the

bound structure and its ideal extended or helical conformation, PepSet was categorized into the following three levels.

- (1) Easy: $RMSD_{\text{bound/helical}}$ or $RMSD_{\text{bound/extended}} \leq 4$ Å
- (2) Medium: $4 \text{ \AA} < (RMSD_{\text{bound/extended}} \text{ and } RMSD_{\text{bound/helical}}) \leq 8$ Å
- (3) Difficult: $(RMSD_{\text{bound/helical}} > 8 \text{ \AA} \text{ and } RMSD_{\text{bound/extended}} > 4 \text{ \AA})$ OR $(RMSD_{\text{bound/helical}} > 4 \text{ \AA} \text{ and } RMSD_{\text{bound/extended}} > 8 \text{ \AA})$

For example, a peptide whose $RMSD_{\text{bound/helical}}$ and $RMSD_{\text{bound/extended}}$ are 5 Å at the same time can be classified as the medium level. Accordingly, on the basis of these classification criteria, all the complexes were divided into 132 easy, 28 medium, and 25 difficult ones (Figure 2A).

Structure Preparation. Since some protein–protein and small molecule docking programs were adopted, the initial

conformations of peptides need to be generated manually. Like pepATTRACT,²⁵ three idealized conformations for each peptide were generated using the Python library PeptideBuilder.²⁶ The backbone dihedral angles and conformation types were set as follows.

- (1) Helical conformation: $\varphi = -57^\circ$, $\psi = -47^\circ$
- (2) Extended conformation: $\varphi = -139^\circ$, $\psi = -135^\circ$
- (3) Polyproline II conformation: $\varphi = -78^\circ$, $\psi = 149^\circ$

Additionally, for the convenience of the determination of the binding sites in local docking, each unbound structure was aligned to the corresponding bound structure on the basis of the residues in the bound protein within 10 Å from the peptide. All nonstandard amino acids in the receptor proteins were modified to standard ones.

Docking Protocol. In this study, 14 docking programs used in protein–peptide docking evaluation were categorized into three protein–protein docking programs, including ZDOCK (version 3.0.2),²⁷ FRODOCK (version 2.1),²⁸ and HawkDock,²⁹ three small molecule docking programs, including GOLD (version 5.3.0),¹¹ Surflex-Dock (version 4221),¹² and AutoDock Vina (version 1.1.2),³⁰ and eight protein–peptide docking programs, including GalaxyPepDock,³ MDockPeP,⁵ HPEPDOCK,⁹ CABS-dock,⁶ pepATTRACT,⁴ DINC (version 2.0),¹⁶ AutoDock CrankPep (ADCP, version 1.0),¹⁷ and HADDOCK peptide docking.¹⁴ The features of the evaluated docking programs are summarized in Table 1, and the key parameter settings for each docking program are described as follows.

GalaxyPepDock. The unbound structures and peptide sequences were uploaded to the GalaxyPepDock server. Due to the limit of protein and peptide lengths, 181 out of 185 complexes could be processed.

ZDOCK. The rotational sampling was set to 6 and the top 100 models for each peptide conformation were retained. In this way, a total of 300 models were obtained and then the top 100 models were extracted according to the ZDOCK scores.

FRODOCK. The unbound structure and three peptide models for each complex were first preprocessed by frodockgrid to generate the potential maps, including the van der Waals, electrostatic, and desolvation potential maps. Then, in the docking and clustering stage, the threshold of the electrostatic map was set to 10 and the maximum number of the clusters was set to 100. Subsequently, the similar model selection strategy for ZDOCK was adopted and the top 100 models were picked out on the basis of the FRODOCK scores.

HawkDock. The unbound structure and three peptide conformations for each complex were uploaded to the HawkDock server. The default parameters of the HawkDock server were used. As the maximal length of protein is limited to 1000 residues, 184 out of 185 complexes were docked successfully. Then, similar to the model selection strategy for ZDOCK, the top 100 models for each peptide conformation were extracted in terms of the HawkDock scores.

MDockPeP. Both global docking and local docking are supported by MDockPeP. In global docking, the unbound structures and peptide sequences were uploaded to its server. The number of the initial peptide models was set to 3. The cutoff of the backbone RMSD was set to 5.5 Å. For docking with standard accuracy (SA), the exhaustiveness value for sampling was set to 100. For docking with high accuracy (HA), considering the computational efficiency and the search exhaustiveness for the peptides with different lengths, the

exhaustiveness value for peptides ranging from 5 to 10 residues was still set to 100, but that for peptides with more than 10 residues increases by 10 for each additional residue. For example, if the peptide contains 16 residues, the value of exhaustiveness will be set to 160. In local docking, the grid box was centered on the cocrystallized peptide ($(x_{\min} + x_{\max})/2$, $(y_{\min} + y_{\max})/2$, $(z_{\min} + z_{\max})/2$). The size of the grid box was set to the maximum value in $((x_{\max} - x_{\min} + 10)$, $(y_{\max} - y_{\min} + 10)$, $(z_{\max} - z_{\min} + 10)$). However, in the actual situations, such a precise size of the grid box is unknown. Therefore, another strategy to determine the size of the grid box based on the peptide length was also adopted by us. The length of the three sides of the grid box was set to (peptide length \times 3.8) Å. The value of 3.8 represents the distance between two adjacent C_α atoms. The other parameters for the local docking were identical to those used in the global docking, except that the parameters of HA were not employed for the local docking whose size of the grid box depended on the peptide length. Since the allowed sizes of protein are 31–1000 residues, 183 out of 185 complexes were calculated successfully.

HPEPDOCK. In global docking, the unbound structures and peptide sequences were uploaded to its server and no parameters needed to be set additionally. In local docking, the binding site was defined as the residues within 5 Å from the peptide.

CABS-Dock. The unbound structures and peptide sequences were uploaded to the CABS-dock server. For docking with SA, the value of the simulation cycles was set to 50. For docking with HA, similar to MDockPeP, for the peptides with more than 10 residues, the value of the simulation cycles increases by 10 for each additional residue and the value of the other peptides was still set to 50. The maximum protein size supported by the server is limited to 500 residues and hence only 173 out of 185 complexes were handled. Moreover, only the top 10 clustering models were assessed by us.

pepATTRACT. Similar to the global docking in the HPEPDOCK server, the pepATTRACT server merely requires the unbound structures and peptide sequences. However, only 184 out of 185 complexes were processed successfully.

GOLD. The definition of the binding site was the same as that employed in HPEPDOCK. The search efficiency of the genetic algorithm was set to “automatic” and the option of “early termination” was switched off. The docking poses were ranked only by the GoldScore scoring function, which performed the best in the LEADS-PEP benchmark.¹⁹ The number of “GA runs” was set to 20 (SA) and (peptide length \times 10) (HA), respectively. Then, according to GoldScore, the conformations for each peptide were collected and reranked.

Surflex-Dock. The protocol file was created on the basis of the cocrystallized peptide and unbound structures using the “proto” mode. The docking calculation was conducted with the “pgeom” mode. On the basis of the Surflex-Dock scores, the models for the three peptide conformations were collected and reranked.

AutoDock Vina. AutoDock-Tools 1.5.6 was utilized to preprocess the unbound structure and three peptide conformations for each complex. The center of the binding site was the same as that of MDockPeP. The size of the grid box was set to $(x_{\max} - x_{\min} + 10)$ Å \times $(y_{\max} - y_{\min} + 10)$ Å \times $(z_{\max} - z_{\min} + 10)$ Å. Moreover, the definition of the binding site based on the peptide length used in MDockPeP was also applied in Vina. Then, the exhaustiveness values were set to 8 (SA) and 100 (HA). Finally, a total of 60 models for each complex were saved and reranked.

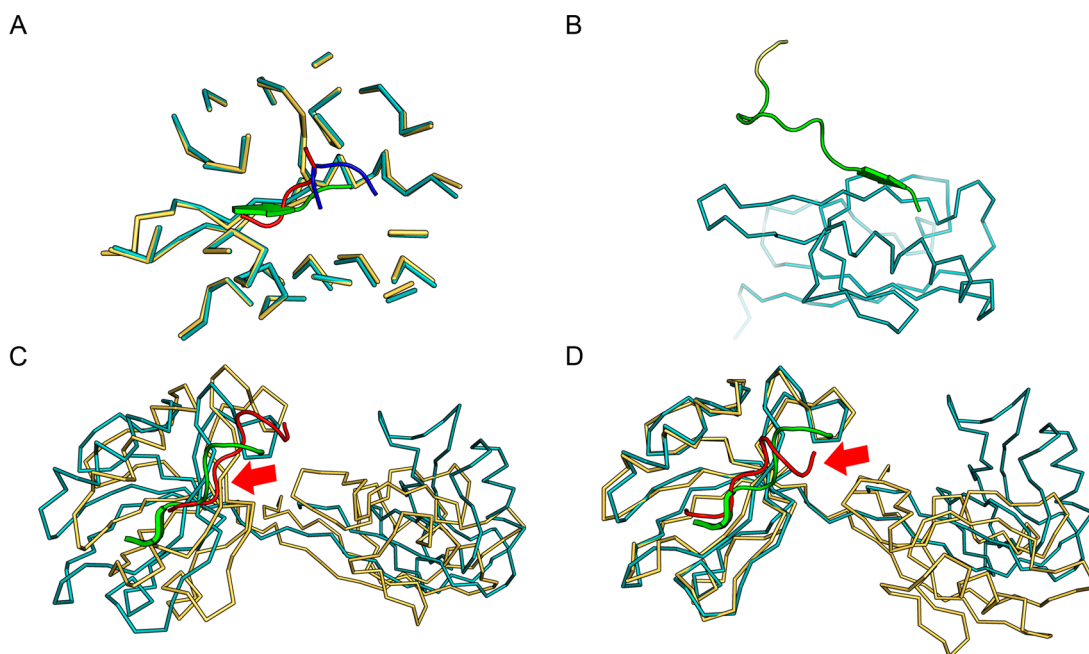


Figure 3. Four examples of the comparison of IL_RMSD with I_RMSD or L_RMSD. The cocrystallized peptide and bound protein structures are colored green and cyan, respectively. The unbound protein structures are colored yellow. The proteins and peptides are illustrated by the ribbon and cartoon, respectively. (A) The red and blue peptides represent the predicted model with I_RMSD = 0.936 Å and I_RMSD = 1.953 Å, respectively. (B) The yellow end represents the residues beyond 10 Å away from the bound protein. Superposition of (C) the entire structures and (D) the binding sites of the bound and unbound proteins, and the red peptide represents the predicted model generated by HADDOCK. The red arrows show the position of peptides.

DINC. Both the sampling method and scoring function in Vina were employed by DINC. The definition of the binding site was also identical to that used in Vina. The value of “num_output” was set to “all”, which means that all the conformations generated by DINC will be returned without clustering. Besides, the values of exhaustiveness and “energy_range” were set to 8 and 3, respectively. The other parameters were set to default. Finally, 183 out of 185 complexes were predicted successfully and the models for the three peptide conformations were merged and reranked according to the Vina scores.

AutoDock CrankPep (ADCP). The docking calculation was executed within a 4 Å padding on every side of the cocrystallized peptide. The value of replicas was set to 80, which consists of 20 simulations started from the helical conformation and 60 simulations started from the extended conformation. Three million *Monte Carlo* steps per residue in the peptide were performed for each replica. Then, the docking poses were clustered and the RMSD cutoff was set to 2.5 Å. Additionally, another definition of the binding site based on the peptide length was also utilized in ADCP. The definition approach was the same as MDockPeP.

HADDOCK Peptide Docking. The unbound structure and three peptide conformations for each complex were uploaded to the expert mode of the HADDOCK server.³¹ The active and passive residues were defined as the residues within 5 Å from the protein and peptide residues, respectively. Moreover, the peptides were docked in the fully flexible way. The numbers of the structures for the rigid body docking, semiflexible refinement and explicit solvent refinement were set to 2000, 400 and 400, respectively. In the clustering stage, the RMSD cutoff for clustering and the minimum cluster size were set to 5 Å and 4, respectively. Finally, according to the HADDOCK scores, the

clustered models for the three peptide conformations were collected and reranked.

Evaluation Metrics. The quality of a predicted protein–peptide model was measured by its RMSD of the ligand in the interface (IL_RMSD) and fraction of native contacts (f_{nat}). IL_RMSD was calculated on the basis of the backbone atoms of the peptide residues within 10 Å from the protein after the optimal superimposition of the protein residues within 10 Å from the peptide. The RMSD calculation was executed using the ProFit program.³² Additionally, in order to further assess the side-chain quality, f_{nat} , the fraction of native contacts between the protein and peptide, is also employed for the assessment. Two residues in the protein and peptide are defined as a contact if any of their heavy atoms are within 4 Å. The criteria for assessment are summarized as follows.

- (1) Near-native prediction: IL_RMSD \leq 4 Å and $f_{\text{nat}} \geq$ 0.2 (peptide length \leq 10); IL_RMSD \leq 5 Å and $f_{\text{nat}} \geq$ 0.2 (peptide length $>$ 10)
- (2) Medium-quality prediction: IL_RMSD \leq 3 Å and $f_{\text{nat}} \geq$ 0.5
- (3) High-quality prediction: IL_RMSD \leq 2 Å and $f_{\text{nat}} \geq$ 0.8

Thus, the success rate, defined as the percentage of the cases with at least one near-native prediction within the top N models, was utilized to assess the performance of docking programs. For example, if the near-native conformations for 74 complexes out of 185 complexes can be found in the top 100 predictions, the success rate at the top 100 level is $74/185 = 40\%$.

RESULTS AND DISCUSSION

Comparison of IL_RMSD with I_RMSD and L_RMSD.

Generally, two kinds of RMSDs, including I_RMSD and L_RMSD, have been used as the criterion to evaluate the quality of the predicted models. I_RMSD is calculated between

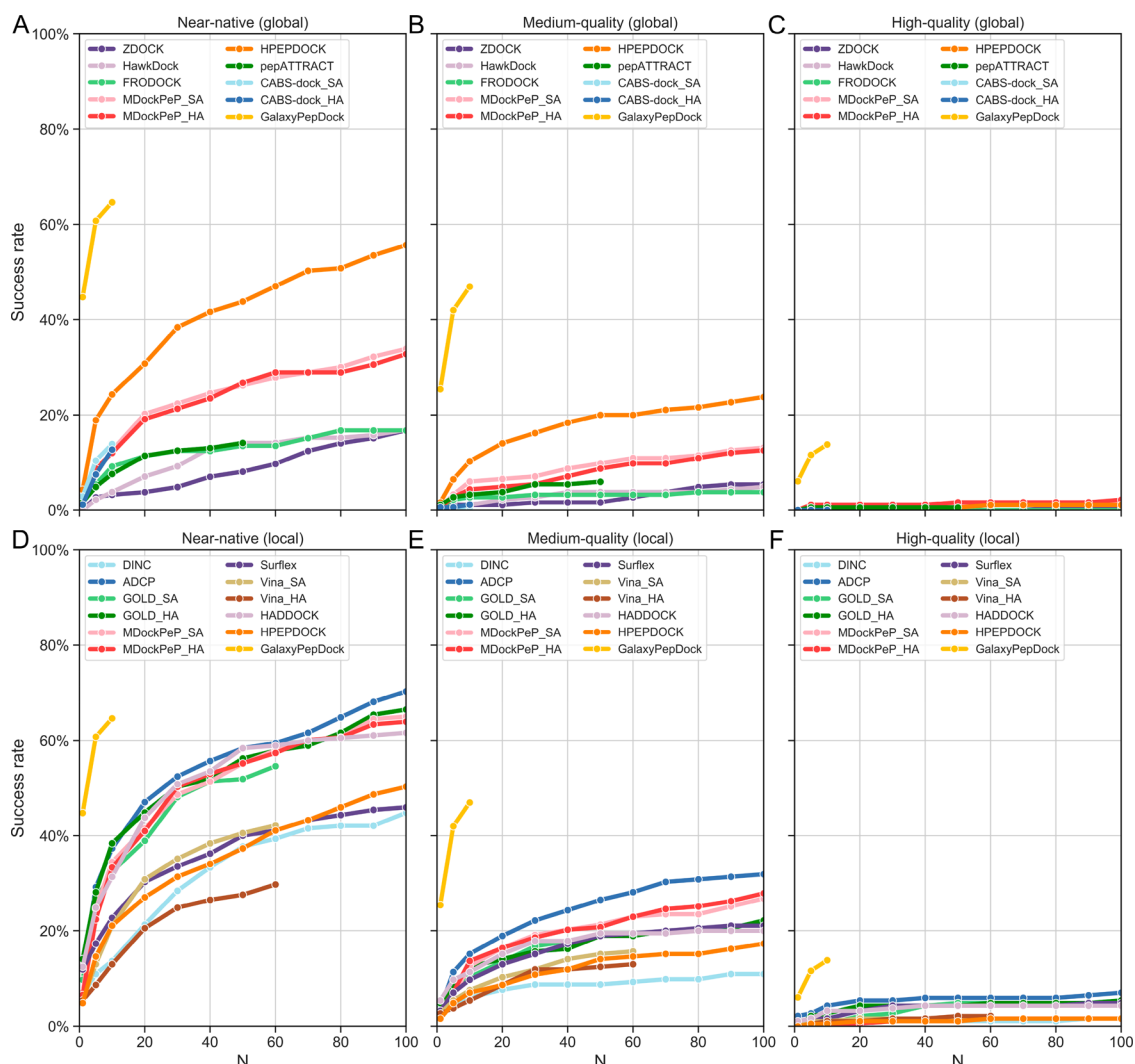


Figure 4. Success rates of global (A–C) and local (D–F) docking programs in the top N predictions for the entire data set.

the predicted model and the experimental structure on the basis of the backbone atoms of the peptide and protein residues within 10 Å of the partner molecules.³³ However, in order to reduce the difficulty of docking, only the RMSD of the binding sites between the unbound and bound structures within 2 Å was collected into our benchmark. Therefore, the effect of peptide deviation will be partially impaired by the good superimposition of the interface residues between the unbound and bound proteins in the I_RMSD calculation, especially for short peptides, because the number of the interface residues of the protein is much more than that of the peptide residues. For clarifying this situation, two near-native models for the 5E33 complex³⁴ based on the criterion of I_RMSD were generated by HPEPDOCK with $I_RMSD = 1.953$ Å ($IL_RMSD = 9.270$ Å, $f_{nat} = 0.269$) and $I_RMSD = 0.936$ Å ($IL_RMSD = 3.946$ Å, $f_{nat} = 0.692$), respectively. Generally, if the I_RMSD between a predicted model and its crystal structure is ≤ 2 Å, this model will be considered as a near-native prediction.¹⁴ Whereas, as shown in Figure 3A, the peptide with $I_RMSD = 1.953$ Å is not supposed to be regarded as a near-native prediction and only the peptide with $I_RMSD = 0.936$ Å is close to the cocrystallized peptide. Furthermore, the difference of the I_RMSDs between these two peptides is about 1 Å, which is quite small. But through the IL_RMSD by excluding the protein residues in the

calculation, only the peptide with $I_RMSD = 0.936$ Å ($IL_RMSD = 3.946$ Å) is regarded as a near-native prediction and the difference of the IL_RMSDs between these two peptides reaches 5.3 Å. Thus, IL_RMSD is a better criterion than I_RMSD in this benchmark.

L_RMSD is calculated on the basis of the backbone atoms of the peptide after the optimal superimposition between the bound and unbound protein structures. But as to some long peptides, it might bring some errors due to the calculation of the RMSD of the entire peptide. Taking 2KOH as an example (Figure 3B),³⁵ the residues colored yellow in the end of the peptide are far from the protein, whose conformations are highly dynamic and unstable. The value of L_RMSD will increase a lot if these residues are considered in the RMSD calculation. However, the binding free energy of PpIs is mainly contributed by some key residues of the peptide that are definitely near the protein.³⁶ As for IL_RMSD , only the peptide residues within 10 Å from the protein are calculated, which can avoid this situation. Moreover, in some proteins, the entire structures of the bound and unbound proteins are quite different, but the structures of their binding sites are similar. As for L_RMSD , the whole protein structures are superimposed before calculation, which will cause some calculation errors to these proteins. For 2KA9 as displayed in Figure 3C,³⁷ the predicted peptide is quite different

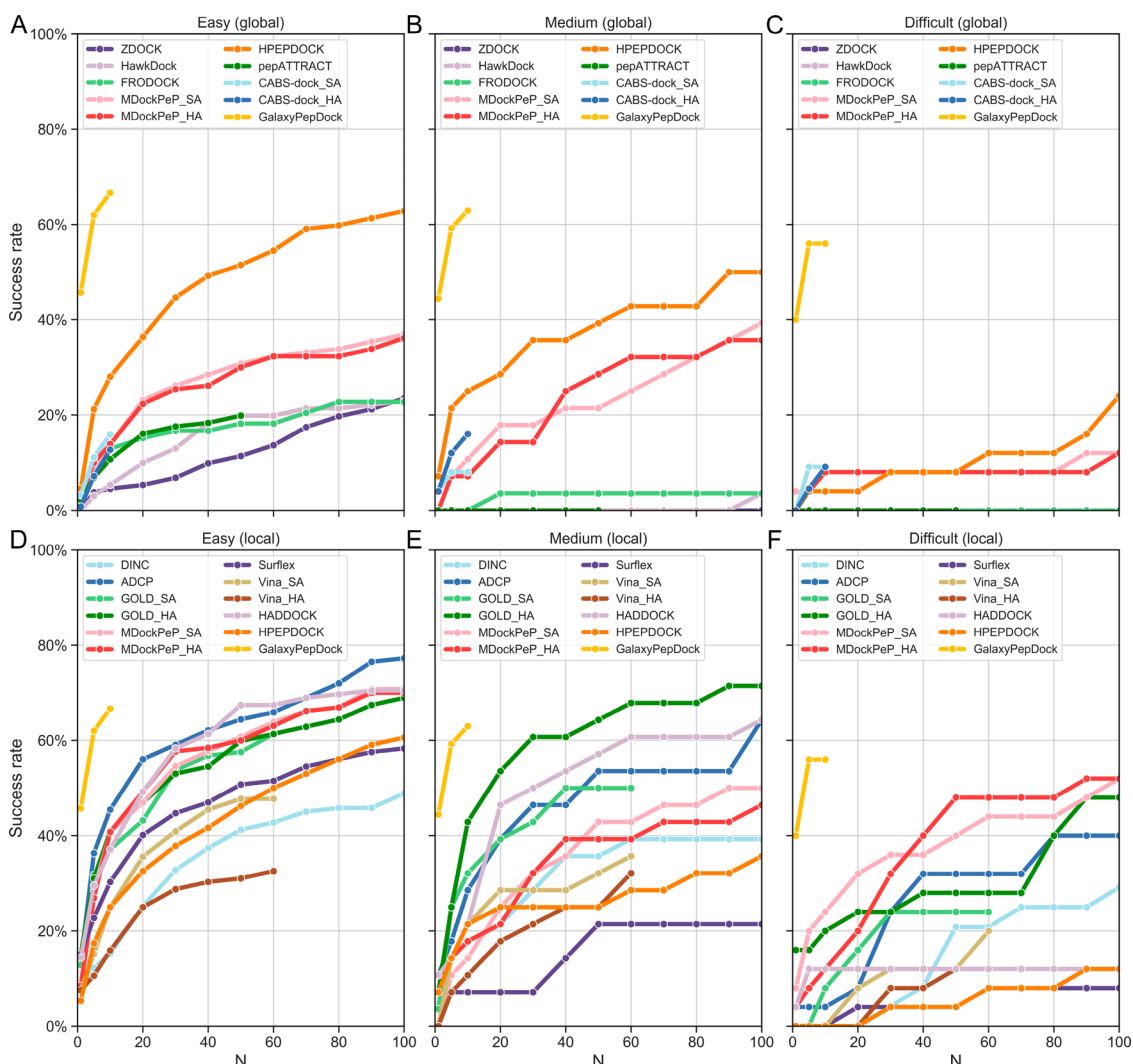


Figure 5. Success rates of global (A–C) and local (D–F) docking programs in the top N predictions for the easy, medium, and difficult subsets.

from the cocrystallized peptide when the entire structures of the bound and unbound proteins are superimposed. Actually, Figure 3D indicates that the binding sites can be well superimposed and the predicted model is supposed to be a near-native prediction. Nevertheless, this error can be avoided if IL_RMSD is used as the criterion because it calculates the RMSD of peptide after the optimal superimposition of the binding site. In summary, IL_RMSD is a better criterion than L_RMSD in the performance evaluation of protein–peptide docking algorithms.

Evaluation of All Docking Programs on the Entire Data Set. Figure 4 shows the success rates of the tested global and local docking programs on the entire data set and the detailed results are summarized in Tables S2 and S3. GalaxyPepDock, the template-based docking approach, performs significantly better than any template-free docking method on the PepSet benchmark. Thus, it is regarded as the target of the performance improvement for the template-free docking methods used in the benchmark.

For global docking, as shown in Figure 4A, HPEPDOCK performs the best with the success rates of 4.3%, 24.3%, and 55.7% at the top 1, 10, and 100 levels, respectively, followed by CABS-dock_SA, CABS-dock_HA, MDockPeP_SA, MDockPeP_HA, FRODOCK, pepATTRACT, HawkDock, and ZDOCK. For pepATTRACT, FRODOCK, HawkDock, and ZDOCK,

only the three idealized conformations for each peptide were docked by the rigid-body docking algorithms, and hence the peptide flexibility cannot be handled well. In contrast, the peptide flexibility can be efficiently considered by HPEPDOCK through an ensemble docking algorithm,⁹ CABS-dock with the Replica Exchange Monte Carlo dynamics,⁶ and MDockPeP using a modified version of AutoDock Vina in the sampling stage.⁵ Additionally, the number of the initial peptide conformations docked by HPEPDOCK reaches up to 1000,⁹ which may be one of the most critical factors for the high success rate of HPEPDOCK. Besides, it can be observed from Figure 4B that the quality of the predictions generated by HPEPDOCK is also notably better than any other methods, suggesting that docking with a variety of initial peptide conformations should be a promising strategy to improve the docking accuracy. Furthermore, HPEPDOCK is more computationally efficient than CABS-dock and MDockPeP. However, as shown in Figure 4C, all methods cannot provide good results in the high-quality prediction.

Figure 4D indicates that, for local docking, ADCP achieves the best predictions with the success rates of 11.9%, 37.3%, and 70.3% at the top 1, 10, and 100 levels, respectively. The performance of the other docking programs follows the following order: GOLD_HA > MDockPeP_SA (local) \approx

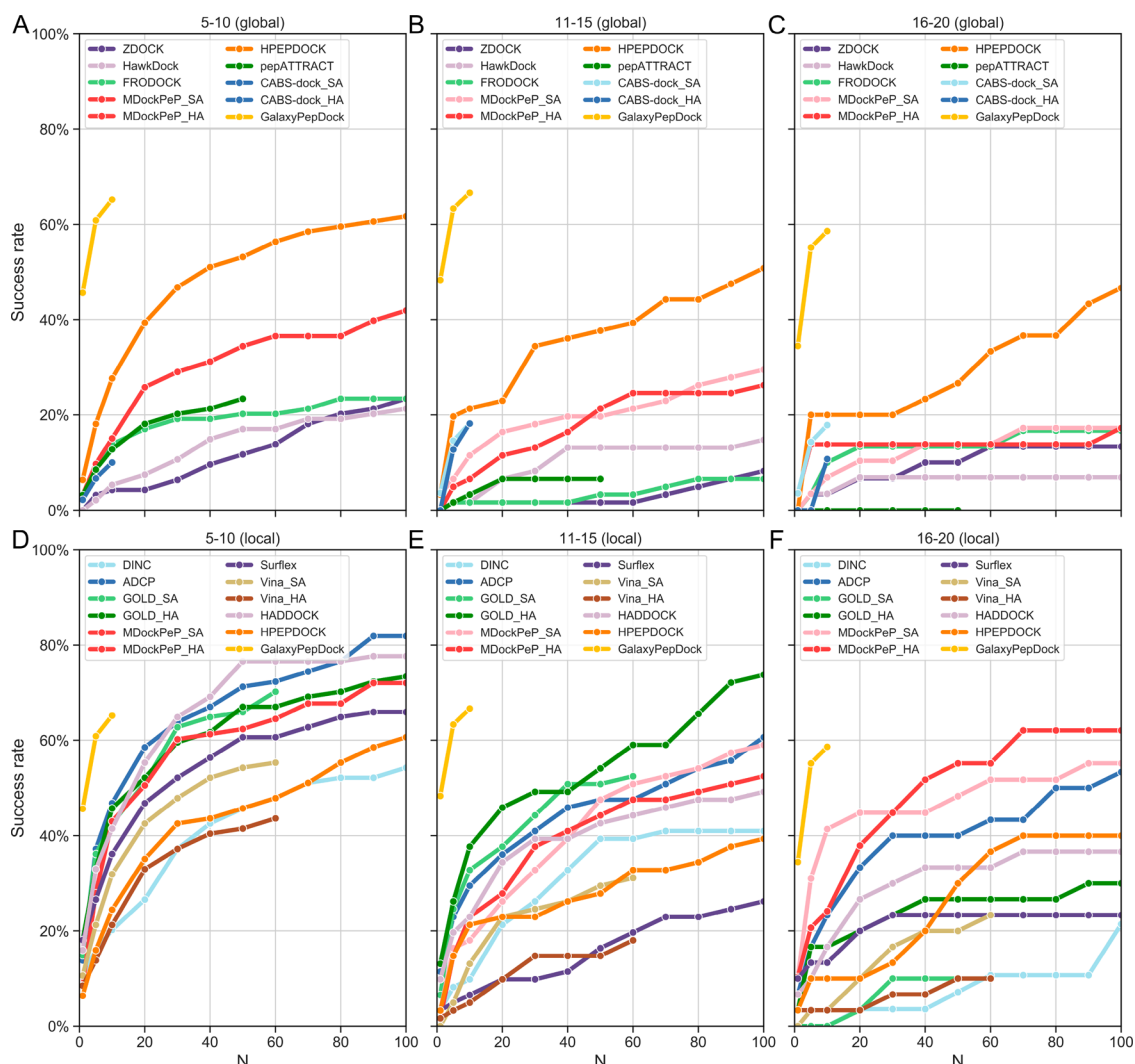


Figure 6. Success rates of global (A–C) and local (D–F) docking programs in the top N predictions for the different peptide length subsets. (A, D) The results of MDockPeP_SA and MDockPeP_HA on the 11–15 subset are identical and thus both of them are colored red.

MDockPeP_HA (local) > HADDOCK > GOLD_SA > Surflex \approx Vina_SA > HPEPDOCK (local) > DINC > Vina_HA. Besides, as illustrated in Figure 4E,F, ADCP also shows better performance than the other local docking algorithms. Generally, compared with global docking, local docking gives remarkably better predictions when a precise binding site is provided. To our surprise, HPEPDOCK (local) performs worse than HPEPDOCK (global) in our benchmark, which is probably caused by the difference between the binding sites of the unbound and bound structures that makes some specified interface residues mislead the sampling of peptide conformations. Among the three small molecule docking programs, GOLD achieves significantly better predictions than Vina and Surflex, even better than most protein–peptide docking algorithms, which is consistent with the evaluation results on a small molecule data set that GOLD supported by the genetic algorithm has the best sampling power.⁵⁸

To investigate the effect of peptide flexibility, the benchmark data set was classified into the easy, medium, and difficult subsets. The results are shown in Figure 5. Overall, as the peptide flexibility increases, the performance of the docking programs gradually decreases. In global docking, similar to the results of the entire data set, as shown in Figure 5A–C,

HPEPDOCK is quite robust and displays the best performance for all the three subsets. The limitations of pepATTRACT, FRODOCK, HawkDock, and ZDOCK in handling peptide flexibility are revealed by the predictions on the medium and difficult subsets. In local docking, as shown in Figure 5D–F, ADCP performs the best for the easy subset, with the success rates of 13.6%, 45.5%, and 77.3% at the top 1, 10, and 100 levels, respectively. However, as for the medium subset, it is defeated by GOLD_HA which reaches the success rates of 7.2%, 42.9%, and 71.4% at the top 1, 10, and 100 levels, respectively. As for the difficult subset, MDockPeP_SA achieves the best predictions and the success rates at the top 1, 10, and 100 levels are 8.0%, 24.0%, and 52%, respectively.

Then, we analyzed the failure cases containing a total of seven structures that cannot be predicted successfully by any docking program, including 1CQG,³⁹ 1VPP,⁴⁰ 2V8C,⁴¹ 4MVI,⁴² 4OUC,⁴³ 5TGI, and 6F6D.⁴⁴ The first reason for prediction failure may be explained by the peptide flexibility. The peptides in 2V8C, 4MVI, 4OUC, 5TGI, and 6F6D bind to the proteins with the “U” or “L” shape, and the docking programs may be not powerful enough to sample such complicated conformations. Second, some peptide residues in 1CQG, 1VPP, and 5TGI are far from the proteins. However, docking programs always try to

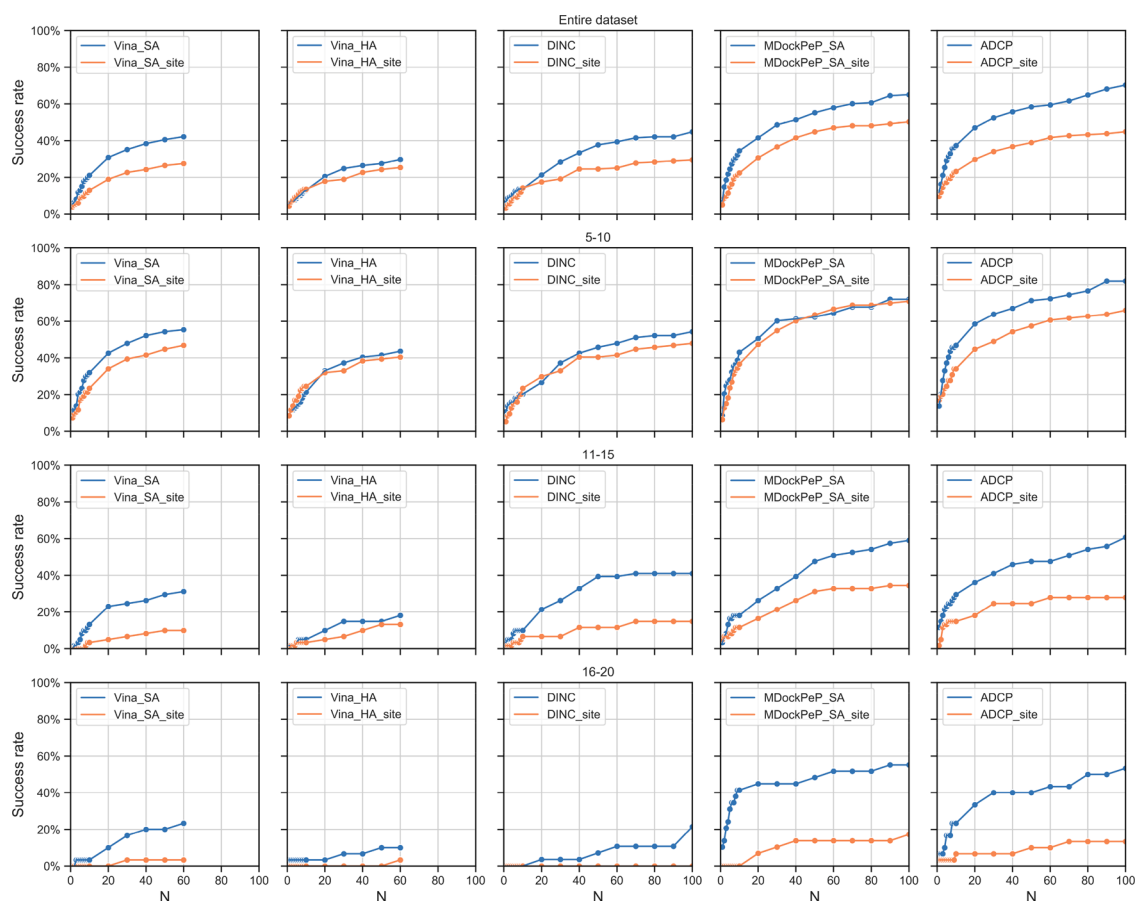


Figure 7. Success rates of the AutoDock or Vina-based docking programs within the top N models for the two different definitions of binding sites. The “site” suffix represents the prediction results for the binding sites defined by the peptide length.

find the peptide conformations that can form compact contacts with proteins, which may trap them into incorrect zones.

Effect of Peptide Length on the Performance of Docking Programs. To further investigate the impact of peptide length on the prediction of the binding modes of protein–peptide complexes, the entire data set was grouped into three subsets with different peptide lengths, i.e., 5–10, 11–15, and 16–20 residues. In global docking, as shown in Figure 6A–C, HPEPDOCK achieves the best predictions for all the three subsets and yields the success rates of 6.4%, 27.7%, and 61.7% for the 5–10 subset, 3.3%, 21.3%, and 50.8% for the 11–15 subset and 0%, 20.0%, and 46.7% for the 16–20 subset at the top 1, 10, and 100 levels, respectively. Moreover, CABS-dock_SA also achieves good predictions on the 11–15 and 16–20 subsets. However, application of the high accuracy settings for CABS-dock does not improve its performance. For MDockPeP, MDockPeP_SA and MDockPeP_HA perform slightly better on the 11–15 and 16–20 subsets, respectively.

In local docking, as shown in Figure 6D–F, ADCP, GOLD_HA, and MDockPeP achieve the best performances on the 5–10, 11–15, and 16–20 subsets, respectively. With the high accuracy settings, the performance of GOLD on the long peptides is improved significantly and it achieves the success rates of 13.1%, 37.7%, and 73.8% on the 11–15 subset at the top 1, 10, and 100 levels, respectively. However, as peptides become longer, its performance drops a lot, which shows the limitation of small molecule docking programs for long peptides. In contrast, the performances of ADCP and MDockPeP are more robust. On the 16–20 subset, MDockPeP_SA and MDockPeP_HA yield

the best predictions at the top 1–30 and top 30–100 levels, respectively.

Impact of the Size of the Binding Site on the Performance of AutoDock or Vina-Based Docking Programs. In local docking, it is difficult to define an exact binding site for peptides, especially for long peptides. As shown in Figure 2B, when the peptides contain more than 10 residues, large difference between the minimum and maximum can be observed and there are four outliers. Taking the peptides with 12 residues as an example, the minimum and maximum values are 18.1 and 37.4 Å, respectively. Furthermore, for the peptides with 19 residues, its outlier reaches 47.5 Å, but its minimum is only 27.1 Å. In a word, the significant fluctuation of the maximum peptide length highlights the difficulty in determining the size of the binding site. Moreover, generally only the information about several key protein residues interacting with peptides is available. Therefore, the influence of the size of the binding site was then evaluated for AutoDock or Vina-based docking programs, including Vina, DINC, MDockPeP and ADCP. As the size of the binding sites was unknown, the determination based on the peptide length was adopted.

As shown in Figure 7, compared with the results of the size of the binding sites defined by the cocrystallized peptides, the success rates of most docking programs drop remarkably on the entire data set. The detailed results are listed in Table S4. Then, the effect of the size of the binding sites on different peptide length data sets is also analyzed. Overall, with the increase of the peptide length, the performance of all docking programs decreases significantly. Figure 7 demonstrates that, for the 5–

10 subset, the performance of MDockPeP and Vina_100 is unchanged but the other methods decline a bit, especially for ADCP. For the 11–15 and 16–20 subsets, the performance of all the docking programs drops a lot, notably for the 16–20 subset whose binding sites usually cover large areas of protein surfaces, sometimes even the whole proteins, which may account for the low success rates. Therefore, when AutoDock or Vina-based docking programs are utilized to dock long peptides, we are supposed to define the binding site more precisely.

CONCLUSION

In the present study, an extensive benchmark data set incorporating 185 complexes with peptide length ranging from 5 to 20 residues was constructed. Based on PepSet, IL_RMSD, a new assessment criterion, proposed by us, was utilized to evaluate 14 docking programs with f_{nat} . The evaluation conclusions can be summarized as follows. (1) Overall, protein–peptide docking algorithms achieve better performance than protein–protein and small molecule docking algorithms. Moreover, docking with diverse initial peptide conformations is a vigorous strategy to improve the docking performance. (2) In global docking, HPEPDOCK shows the best performance. (3) In local docking, ADCP performs the best on the entire data set. As for the performances on the different peptide length subsets, ADCP, GOLD_HA, and MDockPeP yield the best predictions for the 5–10, 11–15, and 16–20 subsets, respectively. (4) The size of the binding site will affect the performance of AutoDock or Vina-based docking programs, and hence we should pay attention to the settings of the binding site.

All in all, prediction of the binding modes between proteins and peptides with large conformational changes still remains a challenge. We expect that our work could provide some valuable clues to the selection and development of improved protein–peptide docking algorithms.

ASSOCIATED CONTENT

Supporting Information

The Supporting Information is available free of charge at <https://pubs.acs.org/doi/10.1021/acs.jctc.9b01208>.

Table S1, summary of the data set; Table S2, ranks given by the global docking programs and GalaxyPepDock for the entire data set; Table S3, ranks given by the local docking programs for the entire data set; Table S4, ranks given by AutoDock or Vina-based docking programs with the binding sites defined by the peptide length (PDF)

AUTHOR INFORMATION

Corresponding Authors

Dongsheng Cao – Xiangya School of Pharmaceutical Sciences, Central South University, Changsha 410013, Hunan, China; orcid.org/0000-0003-3604-3785; Phone: +86-571-8820-8412; Email: oriental-cds@163.com

Tingjun Hou – Innovation Institute for Artificial Intelligence in Medicine of Zhejiang University, College of Pharmaceutical Sciences, Zhejiang University, Hangzhou 310058, Zhejiang, China; State Key Lab of CAD&CG, Zhejiang University, Hangzhou 310058, Zhejiang, China; orcid.org/0000-0001-7227-2580; Phone: +86-571-8820-8412; Email: tingjunhou@zju.edu.cn

Authors

Gaoqi Weng – Innovation Institute for Artificial Intelligence in Medicine of Zhejiang University, College of Pharmaceutical Sciences, Zhejiang University, Hangzhou 310058, Zhejiang, China

Junbo Gao – Innovation Institute for Artificial Intelligence in Medicine of Zhejiang University, College of Pharmaceutical Sciences, Zhejiang University, Hangzhou 310058, Zhejiang, China

Zhe Wang – Innovation Institute for Artificial Intelligence in Medicine of Zhejiang University, College of Pharmaceutical Sciences, Zhejiang University, Hangzhou 310058, Zhejiang, China

Ercheng Wang – Innovation Institute for Artificial Intelligence in Medicine of Zhejiang University, College of Pharmaceutical Sciences, Zhejiang University, Hangzhou 310058, Zhejiang, China

Xueping Hu – Innovation Institute for Artificial Intelligence in Medicine of Zhejiang University, College of Pharmaceutical Sciences, Zhejiang University, Hangzhou 310058, Zhejiang, China

Xiaojun Yao – State Key Laboratory of Quality Research in Chinese Medicine, Macau Institute for Applied Research in Medicine and Health, Macau University of Science and Technology, Taipa, Macau (SAR), China

Complete contact information is available at: <https://pubs.acs.org/10.1021/acs.jctc.9b01208>

Notes

The authors declare no competing financial interest.

ACKNOWLEDGMENTS

This work was financially supported by the National Key R&D Program of China (2016YFA0501701), the National Natural Science Foundation of China (21575128, and 81773632), and Zhejiang Provincial Natural Science Foundation of China (LZ19H300001).

REFERENCES

- (1) Petsalaki, E.; Russell, R. B. Peptide-mediated interactions in biological systems: new discoveries and applications. *Curr. Opin. Biotechnol.* **2008**, *19*, 344–350.
- (2) Zhou, P.; Li, B.; Yan, Y.; Jin, B.; Wang, L.; Huang, S. Y. Hierarchical Flexible Peptide Docking by Conformer Generation and Ensemble Docking of Peptides. *J. Chem. Inf. Model.* **2018**, *58*, 1292–1302.
- (3) Lee, H.; Heo, L.; Lee, M. S.; Seok, C. GalaxyPepDock: a protein-peptide docking tool based on interaction similarity and energy optimization. *Nucleic Acids Res.* **2015**, *43*, W431–W435.
- (4) de Vries, S. J.; Rey, J.; Schindler, C. E. M.; Zacharias, M.; Tuffery, P. The pepATTRACT web server for blind, large-scale peptide-protein docking. *Nucleic Acids Res.* **2017**, *45*, W361–W364.
- (5) Xu, X. J.; Yan, C. F.; Zou, X. Q. MDockPeP: An ab-initio protein-peptide docking server. *J. Comput. Chem.* **2018**, *39*, 2409–2413.
- (6) Kurcinski, M.; Jamroz, M.; Blaszczyk, M.; Kolinski, A.; Kmiecik, S. CABS-dock web server for the flexible docking of peptides to proteins without prior knowledge of the binding site. *Nucleic Acids Res.* **2015**, *43*, W419–W424.
- (7) Porter, K. A.; Xia, B.; Beglov, D.; Bohnuud, T.; Alam, N.; Schueler-Furman, O.; Kozakov, D. ClusPro PeptiDock: efficient global docking of peptide recognition motifs using FFT. *Bioinformatics* **2017**, *33*, 3299–3301.
- (8) Alam, N.; Goldstein, O.; Xia, B.; Porter, K. A.; Kozakov, D.; Schueler-Furman, O. High-resolution global peptide-protein docking

using fragments-based PIPER-FlexPepDock. *PLoS Comput. Biol.* **2017**, *13*, e1005905.

(9) Zhou, P.; Jin, B. W.; Li, H.; Huang, S. Y. HPEPDOCK: a web server for blind peptide-protein docking based on a hierarchical algorithm. *Nucleic Acids Res.* **2018**, *46*, W443–W450.

(10) Rentszsch, R.; Renard, B. Y. Docking small peptides remains a great challenge: an assessment using AutoDock Vina. *Briefings Bioinf.* **2015**, *16*, 1045–1056.

(11) Jones, G.; Willett, P.; Glen, R. C.; Leach, A. R.; Taylor, R. Development and validation of a genetic algorithm for flexible docking. *J. Mol. Biol.* **1997**, *267*, 727–748.

(12) Jain, A. N. Surflex-Dock 2.1: robust performance from ligand energetic modeling, ring flexibility, and knowledge-based search. *J. Comput.-Aided Mol. Des.* **2007**, *21*, 281–306.

(13) Antes, I. DynaDock: A new molecular dynamics-based algorithm for protein-peptide docking including receptor flexibility. *Proteins: Struct., Funct., Genet.* **2010**, *78*, 1084–1104.

(14) Trellet, M.; Melquiond, A. S. J.; Bonvin, A. M. J. A Unified Conformational Selection and Induced Fit Approach to Protein-Peptide Docking. *PLoS One* **2013**, *8*, e58769.

(15) Lamiable, A.; Thevenet, P.; Rey, J.; Vavrusa, M.; Derreumaux, P.; Tuffery, P. PEP-FOLD3: faster de novo structure prediction for linear peptides in solution and in complex. *Nucleic Acids Res.* **2016**, *44*, W449–W454.

(16) Antunes, D. A.; Moll, M.; Devaurs, D.; Jackson, K. R.; Lizee, G.; Kaviraki, L. E. DINC 2.0: A New Protein-Peptide Docking Webserver Using an Incremental Approach. *Cancer Res.* **2017**, *77*, e55–e57.

(17) Zhang, Y.; Sanner, M. AutoDock CrankPep: Combining folding and docking to predict protein-peptide complexes. *Bioinformatics* **2019**, *35*, 5121–5127.

(18) Zhang, Y.; Sanner, M. F. Docking Flexible Cyclic Peptides with AutoDock CrankPep. *J. Chem. Theory Comput.* **2019**, *15*, 5161–5168.

(19) Hauser, A. S.; Windshugel, B. LEADS-PEP: A Benchmark Data Set for Assessment of Peptide Docking Performance. *J. Chem. Inf. Model.* **2016**, *56*, 188–200.

(20) Agrawal, P.; Singh, H.; Srivastava, H. K.; Singh, S.; Kishore, G.; Raghava, G. P. S. Benchmarking of different molecular docking methods for protein-peptide docking. *BMC Bioinf.* **2019**, *19*, 426.

(21) Janin, J. Assessing predictions of protein-protein interaction: the CAPRI experiment. *Protein Sci.* **2005**, *14*, 278–283.

(22) (a) Yu, J.; Andreani, J.; Ochsenbein, F.; Guerois, R. Lessons from (co-)evolution in the docking of proteins and peptides for CAPRI Rounds 28–35. *Proteins: Struct., Funct., Genet.* **2017**, *85*, 378–390.

(b) Schindler, C. E. M.; de Beauchene, I. C.; de Vries, S. J.; Zacharias, M. Protein-protein and peptide-protein docking and refinement using ATTRACT in CAPRI. *Proteins: Struct., Funct., Genet.* **2017**, *85*, 391–398. (c) Xu, X.; Qiu, L.; Yan, C.; Ma, Z.; Grinter, S. Z.; Zou, X. Performance of MDockPP in CAPRI rounds 28–29 and 31–35 including the prediction of water-mediated interactions. *Proteins: Struct., Funct., Genet.* **2017**, *85*, 424–434.

(23) Wen, Z.; He, J.; Tao, H.; Huang, S. Y. PepBDB: a comprehensive structural database of biological peptide-protein interactions. *Bioinformatics* **2019**, *35*, 175–177.

(24) Rose, P. W.; Prlic, A.; Altunkaya, A.; Bi, C.; Bradley, A. R.; Christie, C. H.; Costanzo, L. D.; Duarte, J. M.; Dutta, S.; Feng, Z.; Green, R. K.; Goodsell, D. S.; Hudson, B.; Kalro, T.; Lowe, R.; Peisach, E.; Randle, C.; Rose, A. S.; Shao, C.; Tao, Y. P.; Valasatava, Y.; Voigt, M.; Westbrook, J. D.; Woo, J.; Yang, H.; Young, J. Y.; Zardecki, C.; Berman, H. M.; Burley, S. K. The RCSB protein data bank: integrative view of protein, gene and 3D structural information. *Nucleic Acids Res.* **2017**, *45*, D271–D281.

(25) Schindler, C. E. M.; de Vries, S. J.; Zacharias, M. Fully Blind Peptide-Protein Docking with pepATTRACT. *Structure* **2015**, *23*, 1507–1515.

(26) Tien, M. Z.; Sydykova, D. K.; Meyer, A. G.; Wilke, C. O. PeptideBuilder: A simple Python library to generate model peptides. *PeerJ* **2013**, *1*, e80.

(27) Pierce, B. G.; Hourai, Y.; Weng, Z. Accelerating protein docking in ZDOCK using an advanced 3D convolution library. *PLoS One* **2011**, *6*, e24657.

(28) Ramirez-Aportela, E.; Lopez-Blanco, J. R.; Chacon, P. FRODOCK 2.0: fast protein-protein docking server. *Bioinformatics* **2016**, *32*, 2386–2388.

(29) Weng, G.; Wang, E.; Wang, Z.; Liu, H.; Zhu, F.; Li, D.; Hou, T. HawkDock: a web server to predict and analyze the protein-protein complex based on computational docking and MM/GBSA. *Nucleic Acids Res.* **2019**, *47*, W322–W330.

(30) Trott, O.; Olson, A. J. AutoDock Vina: improving the speed and accuracy of docking with a new scoring function, efficient optimization, and multithreading. *J. Comput. Chem.* **2009**, *31*, 455–461.

(31) van Zundert, G. C. P.; Rodrigues, J.; Trellet, M.; Schmitz, C.; Kastriitis, P. L.; Karaca, E.; Melquiond, A. S. J.; van Dijk, M.; de Vries, S. J.; Bonvin, A. The HADDOCK2.2 Web Server: User-Friendly Integrative Modeling of Biomolecular Complexes. *J. Mol. Biol.* **2016**, *428*, 720–725.

(32) McLachlan, A. D. Rapid comparison of protein structures. *Acta Crystallogr., Sect. A: Cryst. Phys., Diff., Theor. Gen. Crystallogr.* **1982**, *38*, 871–873.

(33) Yan, C.; Xu, X.; Zou, X. Fully Blind Docking at the Atomic Level for Protein-Peptide Complex Structure Prediction. *Structure* **2016**, *24*, 1842–1853.

(34) Kumar, P.; Reithofer, V.; Reisinger, M.; Wallner, S.; Pavkov-Keller, T.; Macheroux, P.; Gruber, K. Substrate complexes of human dipeptidyl peptidase III reveal the mechanism of enzyme inhibition. *Sci. Rep.* **2016**, *6*, 23787.

(35) Tyler, R. C.; Peterson, F. C.; Volkman, B. F. Distal interactions within the par3-VE-cadherin complex. *Biochemistry* **2010**, *49*, 951–957.

(36) London, N.; Movshovitz-Attias, D.; Schueler-Furman, O. The structural basis of peptide-protein binding strategies. *Structure* **2010**, *18*, 188–199.

(37) Wang, W.; Weng, J.; Zhang, X.; Liu, M.; Zhang, M. Creating conformational entropy by increasing interdomain mobility in ligand binding regulation: a revisit to N-terminal tandem PDZ domains of PSD-95. *J. Am. Chem. Soc.* **2009**, *131*, 787–796.

(38) Wang, Z.; Sun, H.; Yao, X.; Li, D.; Xu, L.; Li, Y.; Tian, S.; Hou, T. Comprehensive evaluation of ten docking programs on a diverse set of protein-ligand complexes: the prediction accuracy of sampling power and scoring power. *Phys. Chem. Chem. Phys.* **2016**, *18*, 12964–12975.

(39) Qin, J.; Clore, G. M.; Kennedy, W. P.; Kuszewski, J.; Gronenborn, A. M. The solution structure of human thioredoxin complexed with its target from Ref-1 reveals peptide chain reversal. *Structure* **1996**, *4*, 613–620.

(40) Wiesmann, C.; Christinger, H. W.; Cochran, A. G.; Cunningham, B. C.; Fairbrother, W. J.; Keenan, C. J.; Meng, G.; de Vos, A. M. Crystal structure of the complex between VEGF and a receptor-blocking peptide. *Biochemistry* **1998**, *37*, 17765–17772.

(41) Kursula, P.; Kursula, I.; Massimi, M.; Song, Y. H.; Downer, J.; Stanley, W. A.; Witke, W.; Wilmanns, M. High-resolution structural analysis of mammalian profilin 2a complex formation with two physiological ligands: the formin homology 1 domain of mDia1 and the proline-rich domain of VASP. *J. Mol. Biol.* **2008**, *375*, 270–290.

(42) Rauth, S.; Hinz, D.; Borger, M.; Uhrig, M.; Mayhaus, M.; Riemenschneider, M.; Skerra, A. High-affinity Anticalins with aggregation-blocking activity directed against the Alzheimer beta-amyloid peptide. *Biochem. J.* **2016**, *473*, 1563–1578.

(43) Maiolica, A.; de Medina-Redondo, M.; Schoof, E. M.; Chaikuad, A.; Villa, F.; Gatti, M.; Jeganathan, S.; Lou, H. J.; Novy, K.; Hauri, S.; Toprak, U. H.; Herzog, F.; Meraldi, P.; Penegolo, L.; Turk, B. E.; Knapp, S.; Lindner, R.; Aebbersold, R. Modulation of the chromatin phosphoproteome by the Haspin protein kinase. *Mol. Cell. Proteomics* **2014**, *13*, 1724–1740.

(44) Jones, S. E.; Olsen, L.; Gajhede, M. Structural Basis of Histone Demethylase KDM6B Histone 3 Lysine 27 Specificity. *Biochemistry* **2018**, *57*, 585–592.